Preferred citation: N. Yan and M.T. Kortschot. Micromechanical modelling of tear strength in kraft and TMP papers. In **The Fundametals of Papermaking Materials**, *Trans. of the XIth Fund. Res. Symp. Cambridge, 1997*, (C.F. Baker, ed.), pp 1249–1271, FRC, Manchester, 2018. DOI: 10.15376/frc.1997.2.1249.

Micromechanical Modelling of Tear Strength in Kraft and TMP Papers

N. Yan and M. T. Kortschot

Department of Chemical Engineering and

Applied Chemistry and

the Pulp & Paper Centre

University of Toronto

Abstract

In this study, a mechanistic model was developed for the Elmendorf tear strength of paper based on the fundamental physics of the tear process. In the model, the tear strength was calculated as the sum of fibre fracture energy and fibre pull-out energy. The model also included statistical considerations, such as the distribution of fibre lengths. Through dimensional analysis, a "dimensionless tear index" was identified and was found to be a universal function of three dimensionless parameters. Using a bond strength obtained through non-linear regression analyses on a particular experimental data set, the model was validated with other sets of data. It was found that the model gave good quantitative predictions of tear strength of kraft papers without the need for adjustable fitting parameters. With a slight modification to account for the role of fines in the furnish, the model was also successfully applied to handsheets made from TMP pulps.

Introduction

For many years, tear strength has been widely used as a key parameter for evaluating the quality of paper. Many converters treat tear strength as the most important property and use a specific tear value as a specification in the purchasing of the paper products. Tear strength is also used to evaluate pulp strength development during refining or beating processes, and process engineers traditionally use tear-tensile plots to adjust refining intensity and specific energy. Therefore, a better understanding of the fundamental physics of the tear process will provide a useful tool for product development and quality control.

Although some mechanistic models for tear strength have been developed [1, 2, 3, 4, 5], there is still some controversy about the energy consumption during tearing: some think the fibre pull-out energy is more significant, while others claim the fibre fracture energy is dominant. Two studies have shown that when a fibre is extracted from a sheet, a significant amount of energy is consumed by friction [6, 7]. However, the energy needed to break the fibre may not be insignificant, as assumed in some previous papers. Therefore, it is concluded that a tear model should take into account both energy consumption mechanisms.

The Tear Model

The model presented here is based on a calculation of fibre pull-out and breakage energy. In order to simplify the derivation, a number of assumptions were made. However, these assumptions only affect the mathematical details of the derivation. The approach itself is quite general.

The fibres are assumed to be elastic with a constant fibre modulus and strength. The fibres have a constant diameter. Both the length weighted fibre length and fibre embedded length are assumed to be uniformly distributed, although other distributions for the weighted fibre length may be used. The bond strength

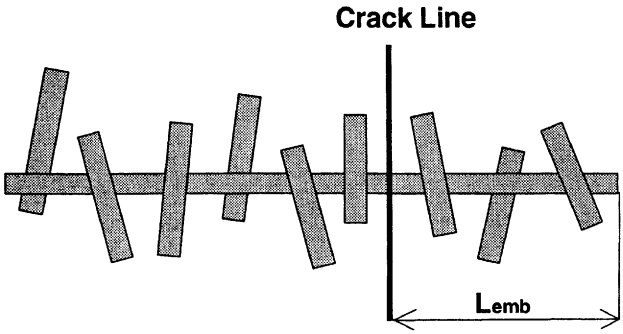

Figure 1: *Schematic of an embedded fibre at the crack.*

(sometimes referred to as the specific bond strength) is assumed to be constant for a given pulping process, however, the RBA is derived for each pulp. Fibre orientation around the crack line is considered to be random. In the model, a fibre is allowed to either break or pull-out. Partial debonding, followed by fracture away from the crack line and subsequent pull-out is not considered.

Fibres are embedded on both sides of the crack plane, as illustrated in Figure 1. The "embedded length" of a fibre is the shorter end of the two parts of the fibre and is considered to be uniformly distributed from $0 - L/2$. The number of fibre bonds along the full fibre and along the shorter embedded end are n_f and n_{emb} respectively. The free fibre length, which is the distance between two bonds, is denoted as L_f.

The force profile along an embedded fibre is assumed to be a linear step function, as shown in Figure 2. This implies that when a load is applied at the crack line, the load is equally distributed among the bonds. When a fibre is short, there are few bonds along the embedded length and the load on the bonds may reach the critical value even though the load in the fibre at the crack line is not high. In this case, the fibre will debond along the embedded length and will be pulled out(fibre b in the figure 2). When a fibre is long, and there are a sufficient number of bonds on each side of the crack line, the

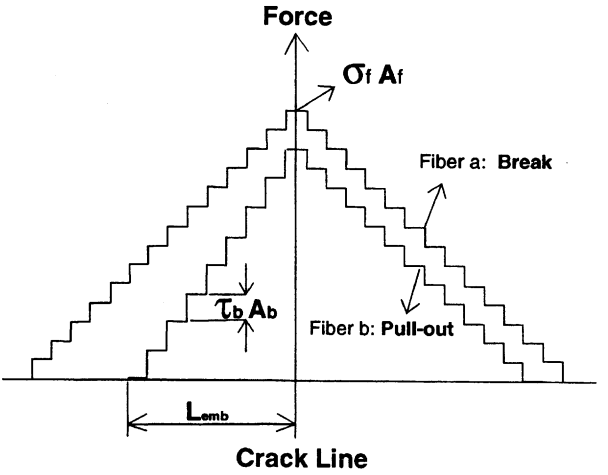

Figure 2: *Force profile of fibres at the crack.*

load in the bonds will be low even when the load at the crack line has already reached the fibre failure load. In this case, the fibre will break at the crack line (fibre a in the figure 2).

When a fibre is broken, the associated energy is calculated based on the following assumptions. A fibre is assumed to break as soon as the central fibre segment is loaded up to the fibre strength. All the elastic energy in the fibre is then released. The elastic energy for a single broken fibre is therefore the sum of the elastic energy of each fibre segment, as shown in Equation 1.

$$\begin{aligned} W_{break} &= \frac{1}{2}(\frac{\sigma_f}{n_{emb}})^2\frac{L_f A_f}{E_f} + \frac{1}{2}(\frac{2\sigma_f}{n_{emb}})^2\frac{L_f A_f}{E_f} + ... \\ &\quad + \frac{1}{2}(\frac{n_{emb}\sigma_f}{n_{emb}})^2\frac{L_f A_f}{E_f} + \frac{1}{2}(\frac{\sigma_f}{n_f - n_{emb}})^2\frac{L_f A_f}{E_f} \\ &\quad + ... + \frac{1}{2}(\frac{(n_f - n_{emb} - 1)\sigma_f}{n_f - n_{emb}})^2\frac{L_f A_f}{E_f} \\ &\approx \frac{\sigma_f^2 A_f L}{6E_f} \end{aligned} \quad (1)$$

When a fibre is pulled out of the network instead of being broken, the energy associated with the fibre includes elastic strain energy, elastic debonding energy and frictional pull-out energy. The elastic energy is calculated using the following equation:

$$\begin{aligned} W^e &= \frac{1}{2}(\frac{\tau_b A_b}{A_f})^2 \frac{L_f A_f}{E_f} + \frac{1}{2}(\frac{2\tau_b A_b}{A_f})^2 \frac{L_f A_f}{E_f} + ... \\ &\quad + \frac{1}{2}(\frac{n_{emb}\tau_b A_b}{A_f})^2 \frac{L_f A_f}{E_f} + \frac{1}{2}(\frac{n_{emb}\tau_b A_b}{(n_f - n_{emb})A_f})^2 \frac{L_f A_f}{E_f} \\ &\quad + ... + \frac{1}{2}(\frac{n_{emb}\tau_b A_b (n_f - n_{emb})}{n_f - n_{emb}})^2 \frac{L_f A_f}{E_f} \\ &\approx \frac{\tau_b {A_b}^2 A_f L_f n_{emb}^3}{6 E_f A_f^2} + \frac{n_{emb}\tau_b {A_b}^2 A_f L_f (n_f - n_{emb})^3}{6 E_f A_f^2 (n_f - n_{emb})^2} \end{aligned} \quad (2)$$

where τ_b is the bond strength. Equation 2 is similar to Equation 1 (the elastic energy of a broken fibre) except that the maximum load at the failure is now $n_{emb}\tau_b A_b$ instead of $\sigma_f A_f$. After debonding, the fibre will be pulled out. The frictional pull-out energy W^p is obtained by assuming a linear step force displacement curve. Results of the single fibre pull-out experiments in paper have shown that a linear force profile is reasonable [6]. τ_f is the frictional pull-out stress.

$$\begin{aligned} W^p &= \tau_f A_b n_{emb} L_f + \tau_f A_b (n_{emb} - 1) L_f + ... + \tau_f A_b L_f \\ &\approx \tau_f A_b L_f {n_{emb}}^2 / 2 \end{aligned} \quad (3)$$

Therefore, the energy consumed by a single pulled out fibre, W_{pull}, is equal to the sum of elastic energy W^e(Equation 2) and pull-out energy W^p(Equation 3).

$$W_{pull} = W^e + W^p \quad (4)$$

Whether the fibre breaks or pulls-out is determined by the relative value of the fibre embedded length and critical embedded length. The critical fibre embedded length is obtained through a simple balance between the force needed to pull the fibre out and the force needed to break the fibre. This calculation assumes that the bonds act cooperatively, and would not be accurate for fibres with many kinks or microcompressions. If n_{crit} denotes the critical number of bonds along the embedded length, then the following equation will describe the force balance:

$$\sigma_f A_f = \tau_b A_b n_{crit} \tag{5}$$

Where, the critical number of bonds, n_{crit} is equal to the ratio between the critical embedded length and the free fibre length, i.e. L_c/L_f.

In summary, there are two classes of fibres in the system after the fibre length distribution is accounted for.

I. When L_{max} is smaller or equal to $2L_c$, all fibres will pull out and no fibres will break.

II. When L_{max} is larger than $2L_c$, fibres

(A) will break if L_{emb} is larger or equal to L_c.

(B) will pull out if L_{emb} is smaller than L_c.

The derivation for the model based on these two cases is as follows:

I. $L_{max} \leq 2L_c$

If the maximum fibre length is smaller than the critical fibre length, all the fibres are pulled out and the energy consumption is given by:

$$W_I = \int_0^{L_{max}} \int_0^{\pi} \int_0^{L/2} W_{pull} P(L_{emb}) dL_{emb} dN_{L,\theta} F_w(L) dL \tag{6}$$

Here, $P(L_{emb})$ and $F_w(L)$ are the probability density functions, PDFs, of the fibre embedded length and weighted average fibre length. Although we may use any practical PDFs for the weighted fibre length distribution, for simplicity we have used the uniform distribution function. The uniform distribution function for the fibre embedded length is given by Equation 7:

$$P(L_{emb}) = \begin{cases} \frac{1}{L/2} & \text{if} \quad 0 \leq L_{emb} \leq L/2, \\ 0 & \text{if} \quad otherwise. \end{cases} \tag{7}$$

The weighted fibre length distribution function is shown in Equation 8.

$$F_w(L) = \begin{cases} \frac{1}{L_{max}} & \text{if} \quad 0 \leq L \leq L_{max}, \\ 0 & \text{if} \quad otherwise. \end{cases} \tag{8}$$

$N_{L,\theta}$ is the number of fibres of angle θ and length L crossing the crack line. For a random network, it is given by:

$$dN_{L,\theta} = \frac{W\ F_w(L)\ dL\ R}{\pi\ \omega} \sin\theta d\theta \tag{9}$$

Here, W is the basis weight of the sheet, R is the sheet width and ω is the fibre coarseness.

After substituting the equation for each term in Equation 6, and integrating, we get the total work for the case I as:

$$W_I = \frac{WR}{\pi\omega}\left[\frac{\tau_f A_b \bar{L}^2}{9L_f} + \frac{{\tau_b}^2 {A_b}^2 \bar{L}^3}{18{L_f}^2 A_f E_f}\right] \tag{10}$$

II. $L_{max} > 2L_c$

When the maximum fibre length is longer than the critical fibre length, there are two subclasses of fibres. (A) Fibres which are shorter than $2L_c$ will be pulled out. The corresponding energy is obtained through Equation 11:

$$W_{IIA} = \int_0^{2L_c} \int_0^{\pi} \int_0^{L/2} W_{pull} P(L_{emb}) dL_{emb} dN_{L,\theta} F_w(L) dL \qquad (11)$$

The difference between Equation 6 and 11 is only in the limits of the fibre length integral. In case II(A), the weighted fibre length is integrated from 0 to $2L_c$ while in case I the integration runs from 0 to L_{max}.

(B) Fibres which are longer than or equal to $2L_c$ will be broken or pulled out depending on their embedded length. Fibres with an embedded length shorter than L_c will be pulled out and the energy consumption may be calculated using Equation 12:

$$W_{IIBa} = \int_{2L_c}^{L_{max}} \int_0^{\pi} \int_0^{L_c} W_{pull} P(L_{emb}) dL_{emb} dN_{L,\theta} F_w(L) dL \qquad (12)$$

When the embedded length is greater than L_c, the fibres are broken and the elastic energy consumption is:

$$W_{IIBb} = \int_{2L_c}^{L_{max}} \int_0^{\pi} \int_{L/2}^{L_c} W_{break} P(L_{emb}) dL_{emb} dN_{L,\theta} F_w(L) dL \qquad (13)$$

The summation of the results of Equations 11, 12 and 13 gives the total tear energy for case II:

$$W_{II} = \frac{WR}{\pi\omega}\left[\frac{\tau_f \sigma_f^3 A_f^3 {L_f}^2}{9\tau_b^3 A_b^2 \bar{L}} + \frac{\tau_f \sigma_f^3 A_f^3 L_f^2}{3\bar{L}\tau_b^3 A_b^2} \ln\left(\frac{\tau_b A_b \bar{L}}{\sigma_f A_f L_f}\right)\right.$$

$$+\frac{\sigma_f^4 A_f^3 L_f^2}{6\tau_b^2 A_b^2 E_f \bar{L}} - \frac{4\sigma_f^3 A_f^2 L_f}{9E_f \tau_b A_b} + \frac{\sigma_f^2 A_f \bar{L}}{3E_f}] \tag{14}$$

Finally, the model for the tear energy absorption is obtained by combining Equations 10 and 14:

$$Work = \begin{cases} \frac{WR}{\pi\omega}[\frac{\tau_f A_b \bar{L}^2}{9L_f} + \frac{\tau_b^2 A_b^2 \bar{L}^3}{18L_f^2 A_f E_f}] & \text{if } L_{max} \leq 2L_c, \\ \frac{WR}{\pi\omega}[\frac{\tau_f \sigma_f^3 A_f^3 L_f^2}{9\tau_b^3 A_b^2 \bar{L}} + \frac{\tau_f \sigma_f^3 A_f^3 L_f^2}{3L\tau_b^3 A_b^2} \ln\left(\frac{\tau_b A_b \bar{L}}{\sigma_f A_f L_f}\right) & \\ +\frac{\sigma_f^4 A_f^3 L_f^2}{6\tau_b^2 A_b^2 E_f \bar{L}} - \frac{4\sigma_f^3 A_f^2 L_f}{9E_f \tau_b A_b} + \frac{\sigma_f^2 A_f \bar{L}}{3E_f}] & \text{if } L_{max} > 2L_c. \end{cases} \tag{15}$$

Normalization

Equation 15 has 11 input variables and a rather complex form. It is extremely difficult to see the functional relationships between the variables. It is also hard to identify the primary variables. However, dimensional analysis can help to simplify the form of the equation and reduce the number of variables. Moreover, dimensional analysis can be used to identify the critical combinations of variables.

The free fibre length for a random sheet assembly of fibres can be approximated as [8]:

$$L_f = \frac{\pi\omega}{4d\rho} \tag{16}$$

The above equation was obtained assuming that fibres are straight cylinders and fibre end effects were neglected. The fibre cross-sectional area is given by $\pi d^2/4$. The fibre bonded area A_b is here assumed to be d^2. This approximation is reasonable for the case of collapsed kraft fibres but will overestimate the

bonded area between fibres because the area where fibres crossing each other may be only partially bonded or partially touching.

Since the logarithmic term of Equation 15 has to be a dimensionless group, this term is therefore defined as one of the dimensionless variables, ϵ. This variable is proportional to the ratio of the fibre length to the critical length. It is a function of the bonding strength and sheet density for handsheets of a chosen furnish. The other two dimensionless variables are suggested simply by inspection of Equation 15. All three dimensionless variables are defined below:

$$\begin{aligned} \epsilon &= \frac{4\rho\tau_b A_b \bar{L}}{\sigma_f \pi^2 d\omega} \propto \frac{L}{L_c} \\ \beta &= \frac{\tau_f}{\tau_b} \\ \alpha &= \frac{\sigma_f}{E_f} \end{aligned} \tag{17}$$

β is the ratio between the frictional pull-out stress and fibre bond strength. The value of β corresponds to the drop in load after the peak in the pull-out curve for a single fibre [6], as shown in Figure 4. β affects the contribution of the pull-out energy to the total tear energy. In previous work by Shallhorn and Karnis, β was assumed to be 1 [2]. α is the fibre elastic strain and affects the contribution of fibre fracture to the tear energy.

By defining three dimensionless parameters and replacing L_f with Equation 16, Equation 15 can be normalized as follows:

$$Work^* = \begin{cases} \frac{\epsilon}{9}\beta + \frac{2\epsilon^2\alpha}{9} & \text{if } \epsilon < \frac{1}{4}, \\ \frac{\beta}{576\epsilon^2} + \frac{\beta}{192\epsilon^2}\ln(4\epsilon) + \frac{\alpha}{384\epsilon^2} - \frac{\alpha}{36\epsilon} + \frac{\alpha}{12} & \text{if } \epsilon \geq \frac{1}{4}. \end{cases} \tag{18}$$

where, $Work^*$ is the normalized work and is obtained by factoring out the rest of the terms in the right side of the equations after using the three dimensionless variables:

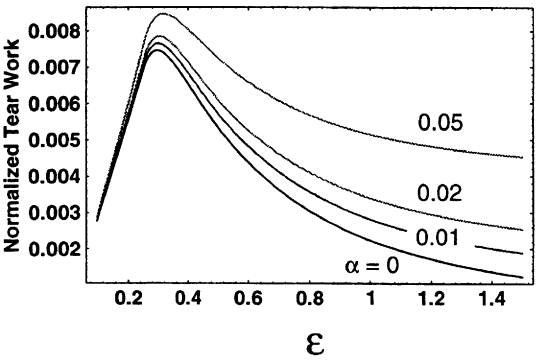

Figure 3: *The normalized tear curves,* $\beta = 0.25$.

$$Work^* = \frac{Work}{\frac{WRd^2\sigma_f\bar{L}}{\omega}} \tag{19}$$

$Work^*$ is the tear index divided by the maximum pull-out energy in the system. The maximum pull-out energy can be obtained by assuming that all fibres are pulled out by a force just slightly smaller than the force needed to break a fibre.

Figure 3 shows the normalized tear curves versus ϵ for different α when $\beta = 0.25$. Clearly, the effect of α is not significant for the range of $1-2\%$. $\beta = 0.25$ is obtained through the single fibre pull-out tests and has been fixed at 0.25 as discussed in [6]. The β value affects the energy contribution from pull-out but does not change the shape of the curve, as illustrated in Figure 4. This figure corresponds to the so called "beating curve": the tear index of paper has been found to pass through a maximum when the degree of bonding is increased by increasing the wet pressing or increasing the degree of refining.

Dimensional analysis

Dimensional analysis is an alternative way to probe some of the findings of the tear model. The tear index of paper is a function of fibre and paper

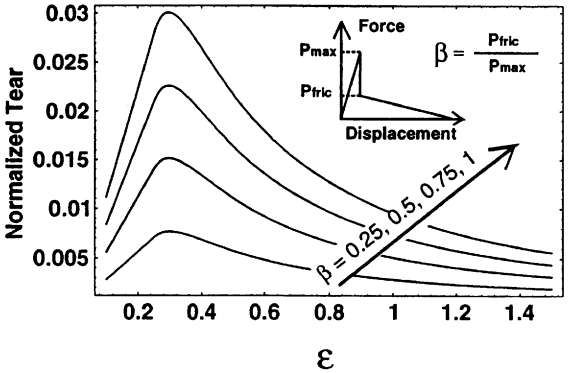

Figure 4: *The normalized tear curves, $\alpha = 1\%$. A schematic of the single fibre pull-out test with a definition of β is included in the inset.*

characteristics:

$$TearIndex = f(L, d, \omega, \sigma_f, E_f, \rho, \tau_b, \tau_f) \tag{20}$$

Based on the Buckingham Π-theorem [9], the dimensionless tear index can be expressed in terms of $(8 - 3 =)$ five independent dimensionless variables. Using L, ω and σ_f as the repeating core variables, we get:

$$\pi_6 = g(\pi_1, \pi_2, \pi_3, \pi_4, \pi_5) \tag{21}$$

where,

$$\pi_1 = \frac{L}{d}$$

$$\pi_2 = \frac{\sigma_f}{E_f}$$

$$\pi_3 = \frac{\tau_b}{\sigma_f}$$

$$\pi_4 = \frac{\tau_f}{\sigma_f}$$

$$\pi_5 = \frac{\rho\, L^2}{\omega}$$

$$\pi_6 = \frac{\omega \, TearIndex}{L^3 \, \sigma_f} \tag{22}$$

Based on the Π-theorem, any multiplication, division, or power of the independent variables (π_i's) can be considered as a new π. Then:

$$Work^* = h(\epsilon, \alpha, \beta, \pi_1, \pi_3) \tag{23}$$

where:

$$\begin{aligned} \epsilon &= \frac{\pi_5 \, \pi_3}{\pi_1} \\ \alpha &= \pi_2 \\ \beta &= \frac{\pi_4}{\pi_3} \\ Work^* &= \pi_6 \, \pi_1^2 \end{aligned}$$

This is partially consistent with the result of our tear model, where the important dimensional groups were identified simply by inspection, with the exception of the two additional variables, π_1 and π_3.

Using SYSTAT software package, regression analysis was performed on experimental data [10] to find out the significance of these two dimensionless variables. Based on the results of this analysis (Table 1), the dimensionless tear index is only a weak function of π_1 and π_3. Meanwhile, the dimensionless tear work was found to be strongly dependent on the ϵ (coefficient of determination is 0.79). This analysis supports the prediction of the tear model, i.e. that dimensionless tear is primarily a function of ϵ, β and α.

Apparent diameter and coarseness for TMP papers

For sheets made from TMP, the effect of fines on mechanical properties is known to be significant. One objective of this modelling effort was to incorporate the effect of fines in the tear model. Fines have several structural functions

Table 1: *The coefficient of determination (r^2) obtained from the regression analysis on experimental data.*

Independent variable	r^2	
	TMP	kraft
π_1	0.25	0.04
π_3	0.01	0.22
ϵ	0.79	0.78

in the sheet depending on their size and type [12]. These effects can be categorized into three mechanisms. Firstly, fines replace long fibres. This yields a reduction in the number of fibres crossing the crack line. The second effect is the increase in bonded area. The addition of high specific surface area fines is believed to increase the degree of bonding in the sheet. The third effect is the increase in sheet density. Based on these effects, the model can be modified for a furnish containing a substantial amount of fines.

The simplest way to modify the model to account for the fines fraction is to introduce two new parameters(the effective diameter and effective coarseness). The effective coarseness is used to describe the portion of fines which only fills in the holes between fibres and does not contribute to bonding in the sheet. These fibres cause the sheet to behave as though the fibres are thickened. The effective coarseness is defined as the original coarseness divided by the fibre fraction.

$$\omega_{eff} = \frac{\omega}{1 - finesfraction} \tag{24}$$

The use of an effective fibre coarseness yields a reduced number of fibres in the sheet at a constant basis weight, and hence reduces the tear strength.

The objective of introducing the effective diameter is to imitate the contribution of the portion of fines which enhance bonding by increasing the bonded

area locally. A higher diameter means a higher bonded area since in our model the bonded area is assumed to be equal to d^2. The effective diameter is defined as follows:

$$d_{eff} = d + 2 \times (\frac{\omega_{eff} - \omega}{\pi \rho_{wall} d}) \tag{25}$$

where, the ρ_{wall} is the fibre cell wall density which is normally found to be constant at around $1.5 g/cm^3$.

Replacing the original fibre diameter and fibre coarseness in the model by the newly defined effective fibre diameter and effective fibre coarseness, the model can be used to describe the effect of fines in the sheet. Note that the density of the sheet is also an input parameter for the model, so that the effect of fines on density will also be accounted for in the tear model.

Model verification

All of the parameters needed for the model, with the exception of the bond strength, can either be measured directly or be roughly estimated. There have been a number of methods developed for measuring bond strength, but none of them is really satisfactory. In this study, non-linear regressions are used to obtain the bond strength.

The data sets used for the regression are taken from Lee [10]. The data sets contain of softwood TMP and kraft pulps of a wide range of species which have been refined to various freenesses. The required parameters for the model are fibre length, width, coarseness, strength, modulus, sheet density and bond strength. The fibre strength was taken as the zero-span tensile strength multiplied by a factor of 8/3 [11]. The fibre modulus was not measured in the study. Instead, the fibre elastic strain, α, was set to be 0.01. According to the literature, α is typically in the range of $1 - 5\%$ for general papermaking fibres. Figure 3 has shown that the effect of α in the range of $0 - 2\%$ is not partic-

ularly significant, so $\alpha = 0.01$ should not introduce a large error. The fibre characteristics of the data sets used for the regression analysis were measured by Lee [10].

Regression for the τ_b value

In order to obtain the numerical value of τ_b, a $Mathematica^R$ program was written to minimize the mean absolute difference between the model predictions and the experimental data. The bond strength corresponding to the minimum average relative error was selected as the optimum τ_b for each pulping process. Although the bond strength(critical shear bond stress) may depend on factors such as external fibrillation and species, it is treated as a constant for each type of pulp. The number of bonds varies however, as a function of density, through Equation 16. Mayhood *et al.* [13] found that the maximum shear stress of fibre to fibre contact did not vary with variations in the nature of the fibre or chemical and mechanical treatments.

The TMP pulps used for the regression consisted of 8 species where each species was refined to three different freeness levels [10]. The kraft pulps were prepared in a batch digester with the same target Kappa number [10].

Results of the regression

Based on nonlinear regressions on 24 TMP and 8 kraft handsheets, the bond strength, τ_b, was found to be $13MPa$ for TMP handsheets and $16MPa$ for kraft handsheets. Using these calculated values of bond strength, the average relative error between the model and the experimental data was about 10% for the TMP and 22% for kraft (see Figures 5).

The ratio between the values of bond strength for kraft and TMP is consistent with what has been reported in the literature. However, the calculated values of the bond strength are substantially higher than those reported in previous studies [13, 14, 16, 17]. The bond strength for fibre/shive bonds of Lobolly pine

holocellulose fibres was found to be in the range of $1-5MPa$ for springwood and $3-10MPa$ for summerwood [17]. The strength of fibre/cellophane bonds has been reported to be in the range of $3-5MPa$ [16]. The bond strength for kraft, CMP, CTMP and TMP estimated by Gorres *et al.* was in the range of $1-6MPa$ [15]. The higher value of bond strength determined through regression could be caused by errors in other input parameters and/or assumptions made in this model. For example, the model did not consider the collapse of the fibres. In the case of the fully collapsed fibres, the potential bonded area is equal to $\pi^2 d^2/4$ which is more than d^2, the value used for the bonded area in the model. An underestimation of the bonded area would result in higher bond strength values.

It should be noted that the data bank used for regression, although quite extensive, covered a relatively small range of furnish characteristics. As a result, no data points lie to the left of the tear energy peak. Furnishes containing short, strong or very weakly bonded fibres are expected to lie to the left of the peak.

The normalization described by Equations 18 to 17 yields a universal tear curve when β and α are fixed. In order to show the advantage of the normalization, α and β were set to be 0.01 and 0.25 respectively.

Application of the model

Using regression analysis, the τ_b value obtained for TMP and kraft pulps were $13MPa$ and $16MPa$ respectively. The model can now be tested with new experimental data.

Two sets of experimental data reported in the literature[18, 19] were used to examine the model predictions. The pulp properties for the data sets are listed in [18], [19]. The experiments carried out by Gurnagul *et al.* [18] used bleached and unbleached hardwood kraft of six different species. Pulps for each species had two beating conditions:unbeaten and beaten at 11000 revs. The studies done by Kazi [19] used mature black spruce unbleached kraft pulps with six different levels of beating. Handsheets of pulps at each beating level were wet

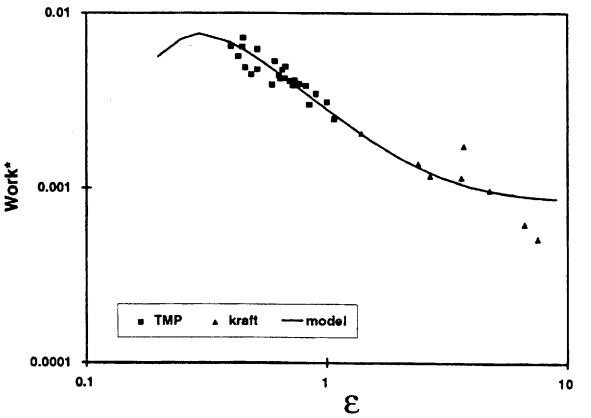

Figure 5: *The universal curve for TMP and kraft pulps. Experimental data are from [10].*

pressed with four different pressures. The original pulps in Kazi's study were taken from Lee's study, but Kazi's data was not used to fit the values of τ_b.

After substituting the pulp properties from each study into the model and setting $\beta = 0.25$ and $\alpha = 0.01$, the model gave reasonable predictions of the experimental values for tear index. The results are shown in Figure 6. The experimental data produced by Lee were used in the regression analysis to obtain the bond strength value. The model predictions for the experimental data from Gurnagul and Kazi's studies were made with no fitting parameters. The average relative error for the data from Gurnagul is 28% and 37% for data from Kazi.

One important feature of Figure 6 is that although there are large numbers of pulps with a wide range of properties, they fall actually close to one universal curve. This demonstrates the importance of the dimensionless groups which have been identified. Figure 6 supports that there is a universal relationship between $Work^*$ and ϵ as predicted by the model.

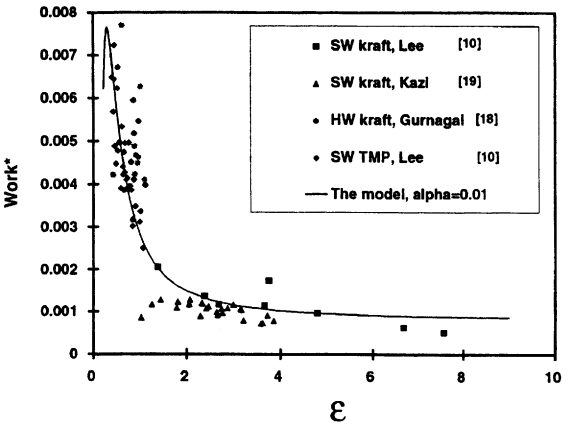

Figure 6: *The application of the tear model for various pulps.*

In Figure 6, $Work^*$ and ϵ share some variables which may introduce cross correlation. However, since $Work^*$ is also a function of tear index and ϵ is dependent on the bond strength and sheet density, the cross correlation caused by the shared variables should have a minor effect on the relationship. Similar dimensionless plots are normally used in many other areas, such as in fluid mechanics.

Another important feature of Figure 6 is that the softwood kraft pulps lie in the highest ϵ region, while the hardwood kraft and softwood TMP pulps clustered in the medium ϵ region. The model also predicts that the initial part of the curve might be populated by hardwood TMP data if they were available.

One trend the model seems to be unable to predict is the effect of wet pressing. In Figure 6, the data points with the highest relative error from the series generated by Kazi is the result of unbeaten and unpressed handsheets.

Figure 7 is a plot of the relative error between the model predictions and the experimental measurements at different wet pressures for six degrees of refining. Clearly, the highest relative error occurred for the unbeaten and unpressed sheets. With increasing wet pressing at the moderate beating levels,

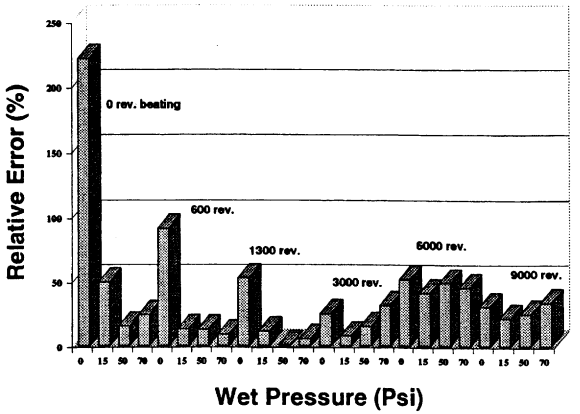

Figure 7: *The relative error in tear index versus wet pressure at various beating levels for Kazi's data.*

the experimental results approach the model predictions, with unpressed sheets representing the largest deviation from the model. For a given wet pressure, increasing the level of beating in the moderate ranges also reduces the relative errors. For the heavily beaten pulps, the effect of wet pressing on the relative error between the model predictions and the experimental results does not show a clear trend. One reason that the model may not have predicted these results properly is the assumption that the bond strength is constant for each pulping process. This assumption does not take into account the effect of wet pressing and degree of beating on the bond strength. Meanwhile, the variable ϵ is a function of density. The sheet density is linearly related to wet pressing, and therefore, the effect of wet pressing and beating should be accounted for in the term describing the number of fibre crossings, (Equation 16). However, for sheets made without wet pressing, the bond strength itself may be much lower than the bond strength obtained through regression on Lee's kraft data. Note that all of Lee's handsheets were made with a standard wet pressure of $50 Psi$. For the heavily beaten pulps, the bond strength could be much higher due to the external fibrillation which can produce mechanical locking of the fibrils.

Conclusions

A mechanistic model was developed for the tear strength of paper. A universal equation was obtained by using the normalization technique. Non-linear regression analysis was performed on 24 TMP and 8 kraft samples. Using the bond strengths obtained from this analysis, the model can make quantitative predictions of tear index for a given furnish. The bond strength for kraft pulps was $16MPa$ and for TMP was $13MPa$. However, the bond strength obtained in this way was higher than the values typically reported in the literature. The discrepancy could have been caused by the errors in the assumptions associated with other input parameters. These errors will be built into the bond strength values through regression analysis. The relative errors for the model predictions and the experimental data used in the regression analysis were 10% and 22% for TMP and kraft pulps respectively.

Using the bond strength values obtained through regression analysis, the model predictions were compared with experimental data from the literature without further parameter adjustments. Most experimental data followed the trend of the model predictions rather well.

A simple, novel approach has also been introduced to take into account the effect of fines. The data of sheets made under various conditions from a wide range of species were lying close to one universal curve as predicted by the model. The relative average error for the model predictions was 28% for the hardwood kraft pulps and 37% for the data from the beating and wet pressing studies on the softwood kraft pulps.

On the universal tear curve, the softwood kraft pulps lay in the region with the highest ϵ while the hardwood kraft and softwood TMP pulps were located in the medium ϵ region. The low ϵ region was not tested with experimental data. It was expected that very poorly bonded or very strong wood pulps would be located in that region. The dimensionless analysis approach has not been applied to paper strength models previously. When plotting the data in terms of dimensionless groups, a single curve relating tear energy to bonding was predicted. The experimental data supports the associated model.

Acknowledgements

The authors would like to acknowledge the financial contribution of the Mechanical and Chemimechanical Wood Pulps Network, a National Network of Centres of Excellence. We are also grateful for the cooperation from Abitibi-Price Inc..

References

[1] Kane, M.W., Beating, fibre length distribution and tear. *Pulp and Paper Magazine of Canada* 61(3) P236 (1960).

[2] Shallhorn, P. and Karnis, A., Tear and tensile strength of mechanical pulps. *Transactions* P92 December (1979).

[3] Karenlampi, P., Retulainen, E. and Kolehmainen, H., Properties of kraft pulps from different forest stands - Theory and experiment. *Nordic Pulp and Paper Research Journal* No. 4 P214 (1994).

[4] Page, D.H., A note on the mechanism of tearing strength. *Tappi* 77(3) P201 (1994).

[5] Yan, N. and Kortschot, M.T., Modelling of out-of-plane tear energy absorption of paper. *Appita* 49(3) P176 (1995).

[6] Yan, N. and Kortschot, M.T., Single fibre pull-out tests and the Elmendorf tear strength of paper. 1997 CPPA annual meeting proceedings (1997).

[7] Davison, R.W., The weak link in paper dry strength. *Tappi J.* 55(4) P567 (1972).

[8] Komori, T. and Makishlma, K., Numbers of fibre-to-fibre contacts in general fibre assemblies. *Textile Research Journal* 47(1) P13 (1977).

[9] Giles, R.V., Evertt, J.B. and Liu, C., Schaum's outline series, Fluid mechanics and hydraulics, Third Edition, McGraw-Hill, Inc. (1994).

[10] Lee, J., Relationships between properties of pulp-fibre and paper. Doctoral Thesis University of Toronto. (1992).

[11] Van Den Akker, J.A., Lathrop, A.L., Voelker, M.H. and Dearth, L.R., Importance of fibre strength to sheet strength, *Tappi* 41(8) P416 (1958).

[12] Silveira, G., Zhang, x., Berry, R. and Wood, J.R., Location of fines in mechanical pulp handsheets using scanning electron microscopy. *JPPS* 22(9) P315 (1996).

[13] Mayhood, C.H., Jr., Kallmes, O.J. and Cauley, M.M., The mechanical properties of paper, Part II. Measured shear strength of individual fibre to fibre contacts. *Tappi* 45(1) P69 (1962).

[14] Thorpe, J.L., Mark, R.E., Eusufzai, A.R.K. and Perkins, R.W., Mechanical properties of fibre bonds, *Tappi* 59(5) P96 (1976).

[15] Gorres, J., Amiri, R., Wood, J. and Karnis, A., The shear bond strength of mechanical pulp fibres. *JPPS* 21(5) P161 (1995).

[16] Mohlin, U-B. Cellulose fibre bonding. *Svensk Papperstidn.* 77(4) P131 (1974).

[17] McIntosh, D.C. and Leopold, B., Bonding strength of individual fibres. Formation and structure of paper, P265, London, British Paper and Board Makers' Assn., (1961).

[18] Gurnagul, N.,Page, D.H. and Seth, R.S., Dry sheet properties of Canadian hardwood kraft pulps. *JPPS* 16(1) P36 (1990).

[19] Kazi, S., The effects of pulp type on the mechanical properties of paper. Master Thesis University of Toronto. (1992).

Transcription of Discussion

Micromechanical modelling of tear strength in kraft and TMP papers

Ning Yan, Paprican, Canada

Christer Fellers, STFI, Sweden

I think it is a very interesting and ambitious theory you presented but I have difficulties with a few things, especially that which addresses the differences between the theory and the true fractography of tear. If you take a piece of paper and tear it, it doesn't tear along an in-plane line - it is more like a delamination type of failure. So I don't think what you model is actually occurring in reality.

Ning Yan

That is true. I agree. Our model is just a simplification of the real fracture process. There are many phenomena going on when a piece of paper is torn. There is delamination. However, in the case of 4-ply tear test, the degree of delamination is smaller in average comparing to 1-ply tear test.
About the comment that the fracture path during the tear does not follow a straight line, I agree with you on this as well. The tear path may tend to pass through some of the low basis weight regions while avoiding high basis weight regions. However, if that is the case, the tear path will be longer than a straight line. The resulting tear energy may be equivalent to energy consumed along a straight line that passes through the mean basis weight regions. This we do not know. We have to make some simplifications in order to construct the model. Therefore, I totally agree with you that the real fracture process is much more complex.

Dr Derek Page, IPST, USA

I agree with Christer. It seems to me that what you've done is to simulate the in-plane tear test not the Elmendorf plane tear test. Now the results from the in-plane and Elmendorf tests differ enormously and so I am not impressed that you get any agreement at all with Elmendorf tear because if you get agreement with Elmendorf tear then I'm afraid you wouldn't get any agreement with in-plane tear results.

Ning Yan

The reason I have chosen Elmendorf tear is because, in my opinion, it is more close to this kind of modelling. The stress field at the crack tip in the Elmendorf mode is perhaps than

the in-plane tear mode. We know that in the in-plane fracture test, the stress is distributed over a quite large region. The effect of neighbouring fibres should be taken into account. In the Elmendorf tear mode, the stress field is perhaps more concentrated at the crack tip. About the fracture process, the idea behind modelling fracture energy based on fibre pull-out and breakage will be the same for the in-plane and Elmendorf (out-of-plane) tear, but each parameter involved in the modelling will have different values.

Derek Page

Could I just make a quick second point. I find it difficult to understand your paper because it doesn't make clear what the relationships are between properties that we all know. For example, supposing you take a well bonded sheet, what is the relationship between work of rupture and fibre strength, keeping everything else constant in the sheet?

Ning Yan

I'm glad you are asking this because in our thesis we also carried out further work that I like to explain to you. If you recall the curve of normalised tear work vs ε when α and β are constants, the curve can be divided into three regions, increasing, decreasing and plateau, depending on the value of ε, which depends on sheet density and bond strength for a given pulp furnish. The relationship between tear and fibre and paper characteristics for each region is shown in the following table. For example, in the second region, which is the decreasing region, the tear index is proportional to fibre strength to a power of around 2. That means 10% increase in fibre strength will give about 20% increase in tear. However, if you are in the first increasing region, fibre strength has no effect on tear. That is what is derived from our model.

Region	ε	**Fibre length**	**Fibre width**	**Fibre coarseness**	**Fibre strength**	**Fibre modulus**	**Sheet density**	**Bond strength**
I	≤ 0.32	L^2	d^3	$1/\omega^2$	0	0	P	0
II	> 0.32 & 3.3	0	d	0	σf^2	0	1/p	$1/\tau_b^2$
III	≥ 3.3	L	d^2	$1/\omega$	σf^2	E	0	0

Ning Yan, PhD thesis, University of Toronto, 1997

Derek Page

Yes, that's useful because that does agree with experimental data.

Ning Yan

The results shown in the above table are found to be rather consistent with observations reported in the literature.

Dr R S Seth, Paprican, Canada

Dr Page has already asked several of the questions I wanted to. Are you aware that the results in the literature are all four ply tear and there is a tremendous difference between four-ply tear and single ply tear for the Elmendorf mode?

Ning Yan

Yes. I applied the model only to the results of 4-ply tear tests. The reason behind this was, as I explained in the previous questions, that the degree of delamination is not as severe as in one ply tear test. Therefore, we think it is more suitable for using the model.

Raj Seth

I am not that sure.

Ning Yan

Perhaps it could be. But at this stage, the data used in the work are all obtained from 4-ply tear tests.